Annals of Nuclear Medicine Vol. 15, No. 3, 301–306, 2001

A basic study on lesion detectability for hot spot imaging of positron emitters with dedicated PET and positron coincidence gamma camera

Hong ZHANG,* Tomio INOUE,* Mei TIAN,*,** Saleh ALYAFEI,* Noboru ORIUCHI,* Nasim KHAN,* Sijin LI** and Keigo ENDO*

*Department of Diagnostic Radiology and Nuclear Medicine, Gunma University School of Medicine, Gunma, Japan
**Department of Nuclear Medicine, First Hospital of Shanxi Medical University, Shanxi, People's Republic of China

The aim of this study was to explore the correlations of detectability and the semi-quantification for hot spot imaging with positron emitters in positron emission tomography (PET) and with a positron coincidence detection system (PCD). Phantom study results for the measurement of the lesion-to-background (L/B) ratio ranged from 2.0 to 30.3, and detectability for hot spot lesion of PET and PCD were performed to correspond to clinical conditions. The detectability and semi-quantitative evaluation of hot spots from 4.4 mm to 36.9 mm in diameter were performed from the PET and PCD images. There were strong correlations between the L/B ratios derived from PET and PCD hot spot images and actual L/B ratios; but the L/B ratio derived from PET was higher than that from PCD with a significant difference of 10% to 54.8%. The detectability of hot spot imaging of PCD was lower than that of PET at 64.8% (PCD) versus 77.8% (PET). Even the actual L/B ratio was 8.0, hot spots more than 10.6 mm in diameter could be clearly identified with PCD imaging. The same identification could be achieved with PET imaging even when the actual L/B ratio was 4.0. This detailed investigation indicated that FDG PCD yielded results comparable to FDG PET on visual analysis and semi-quantitative analysis in detecting hot spots in phantoms, but semi-quantitative analysis of the L/B ratio with FDG PCD was inferior to that with FDG PET and the detectability of PCD in smaller hot spots was significantly poor.

Key words: dedicated PET, positron coincidence gamma camera, detectability, semi-quantification, lesion-to-background ratio

INTRODUCTION

SINCE POSITRON EMISSION TOMOGRAPHY (PET) offers the possibility of investigating the glucose metabolism of tissues *in vivo*, PET with 2-(fluorine-18)fluoro-2-deoxy-D-glucose (FDG) plays an important role in oncology.[1–3] But widespread implementation of PET as a clinical imaging method has been hindered by the high cost of the imaging system, cyclotrons, support laboratories, maintenance and operation.[4] Alternative methods of imaging the 511-keV photons of positron emitters have been sought. Although findings in preliminary studies of malignancies have demonstrated that SPECT study with ^{18}FDG is feasible with a conventional gamma camera fitted with high-energy (511 keV) collimators,[5–7] the limitations of SPECT imaging for detecting small lesions with ^{18}FDG make it unlikely that this method will have much effect on FDG tumor imaging.[5] Recently, dual-head gamma cameras with modified coincidence detection have become available for oncological FDG-PET imaging. These systems provide both higher spatial resolution and system sensitivity than the SPECT system. Several clinical studies reported high detection accuracy for lung lesions with coincidence gamma camera systems that are comparable with PET.[8] But further studies in order to obtain a full understanding of the impact of lesion size and image contrast are needed.[8] Especially in detecting hot lesions

Received October 16, 2000, revision accepted March 3, 2001.
For reprint contact: Hong Zhang, D.M.Sc., Department of Diagnostic Radiology and Nuclear Medicine, Gunma University School of Medicine, 3–39–22 Showa-machi, Maebashi, Gunma 371–8511, JAPAN.
E-mail: zhang@med.gunma-u.ac.jp

Table 1 Brief performance with positron imaging cameras

Cameras	Resolution* (FWHM: mm)	Sensitivity (kcps/kBq/m*l*)	Scatter fraction (%)	NERC	
				(kcps)	(kBq/m*l*)
Prism-2000XP					
2-dimensional	5.7	1.8	22	3.9	0.2
3-dimensional	5.7	9.5	34	3.45	0.05
SET-2400W					
2-dimensional	4.4	7.98	13.1	73.0	28.0
3-dimensional	4.7	48.95	30.1	86.1	5.8

*Reconstructed transaxial resolution at the center of the field of view. PCD: Coincidence gamma camera (Picker, Co., OH). SET-2400W: Dedicated PET (Shimadzu, Co., Kyoto). PCD data were measured within combinations of coincidence events identified by 30% photopeak-Compton scatter window. NERC: Noise-equivalent count rate.

Table 2 Results of detectability limitation for small hot lesion on phantom's reconstructed PET and PCD images

L/B ratio	Hot spot size (Diameter: mm)	
	PET	PCD
2.0	22.5	36.9
4.0	10.6	16.3
6.0	10.6	16.3
8.0	10.6	10.6
9.6	6.3	10.6
13.2	6.3	10.6
17.5	4.4	6.3
23.8	4.4	6.3
30.3	4.4	4.4

with FDG, even FDG imaging has been able to be obtained from PET and PCD, but it is important to understand the correlation between the above two imaging methods: what and how the detectabilities are and change, and how the contrast is affected by lesion size, therefore providing accurate understanding and procedure for hot lesion diagnosis and treatment. The purpose of this study was to evaluate the correlation between FDG-PET and FDG-PCD in detecting small hot lesions with varying lesion sizes and lesion to background uptake (L/B) ratios.

MATERIALS AND METHODS

We chose to use a hot spot phantom (AZ-619-P) study as it is more representative of the imaging quality associated with clinical scanning and easier to use in investigating the influence of lesion size and L/B ratio to the detectability in PET and PCD. All PET and PCD imaging were performed under conventional clinical conditions.

Measurements and image reconstruction

By using a hot spot phantom (AZ-619-P), which is 20 cm diameter 18.5 cm high pool phantom containing six columns inside simulated tumors with diameters of 4.38–36.88 mm, the imaging of PET and PCD were performed by using SET-2400W PET (Shimadzu, Co., Japan) and a Prism-2000XP coincidence camera (Picker, Co., USA).

The whole-body PET scanner SET-2400W has a large axial field of view (20 cm), which consists of 32 rings of 21,504 BGO crystals, giving 63 two-dimensional imaging planes. The Prism-2000XP imaging system consists of two opposite rectangular gamma cameras modified to allow imaging of both single photon and positron emitters. The system is equipped with two 19 mm NaI(Tl) crystals with a transaxial field of view of 508 mm and an axial field of view of 381 mm. A dual-window technique was used to accept the coincidences between photopeak events and photopeak and Compton events. This technique increases the coincidence rate but also results in an increase in scattered and random events.[10] The pre-windows (photopeak 511 keV ± 30%, Compton window 310 keV ± 30%) were adjusted for phantom studies. In the coincidence mode, stray radiation shields are mounted on each detector to decrease radiation from outside the field of view. The performance of SET-2400W and Prism-2000XP was done in our previous study,[9,15] which is summarized in Table 1.

The hot spot phantom was also assessed with X-CT and contrast solution to measure the column diameter in clinical condition.

In the present phantom study, the hot spot phantom contained six hot spots with diameters of 4.38–36.88 mm, which were filled with ^{18}F sodium fluoride solution. The phantom was placed on the bed and centered within the field of view. Nine acquisitions were performed with the concentration adjusted to provide ratios of hot spot activity to background activity of 2:1, 4:1, 6:1, 8:1, 9.6:1, 13.2:1, 17.5:1, 23.8:1 and 30.3:1 for both PET and PCD, respectively, to simulate various clinical situations for detecting hot lesion. Since the experiments were assumed to be under clinical conditions, the concentration of background in the phantom was calculated and set at 3.7 kBq/m*l* (Injection Dose/g), as in the case of a typical clinical administration of 185 MBq FDG administered to a person with a normal weight of 60 kg, and the gravity of the tumor and background muscle was assumed to be 1 g/m*l*.[10]

The simultaneous transmission and emission PET data were acquired in 2D for 8 minutes for the phantom, as

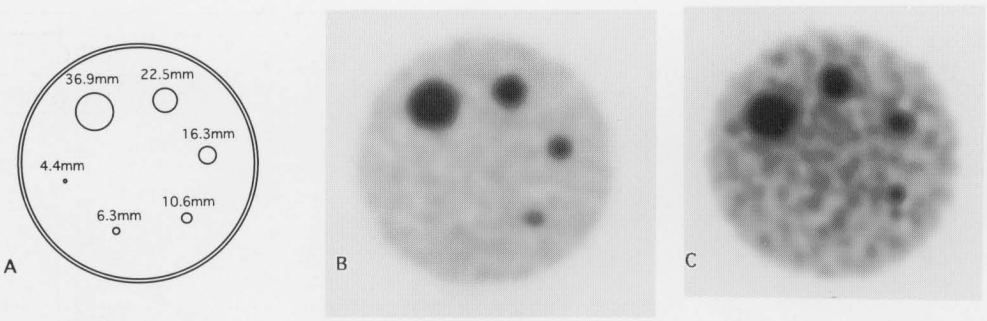

Fig. 1 The line drawing of (A) indicates the relative size and position of hot spot containing FDG solution. Images of the hot spot phantom in 2D PET (B) and PCD (C) scanning with an actual L/B ratio of 8.0.

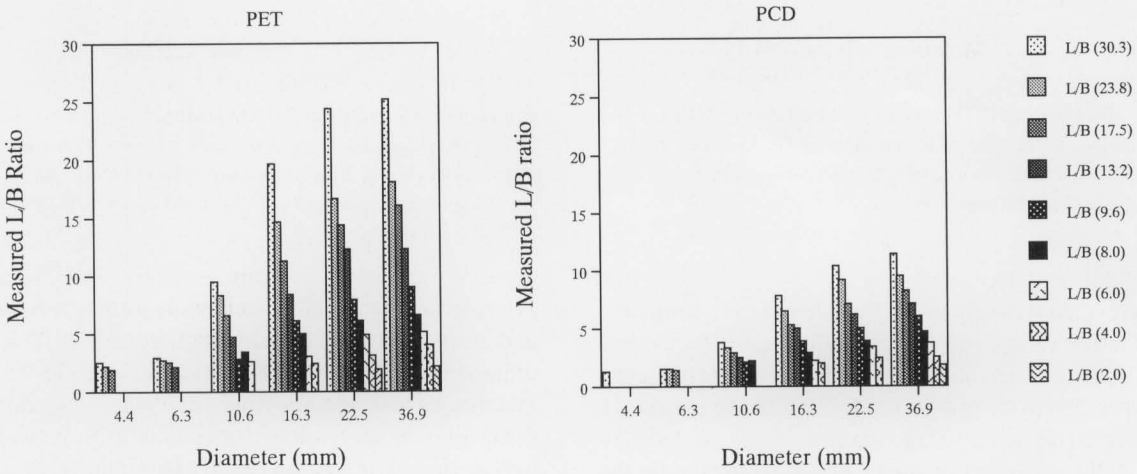

Fig. 2 Correlations between measured L/B ratios of 2D PET and PCD and lesion size ranged from 4.4 mm to 36.9 mm in diameter. PVE was observed in both PET and PCD.

demonstrated in our previous study,[9] showing that simultaneous transmission and emission PET scan had the same feasibility as semi-quantification with 2D transmission corrected emission PET scan. All the emission data underwent measured attenuation correction. The order subsets expectation maximization (OSEM) algorithm was used to reconstruct attenuation-corrected PET emission data. The OSEM algorithm with the number of subsets equal to 16 and iterations equal to 1, was used for 2D image reconstruction. The images were reconstructed in a 128 × 128 matrix with a Butterworth filter with a cutoff level of 0.35 cycle/pixel and order 2. Decay and dead time correction was automatically performed during the acquisition step.

The PCD imaging of the phantom was performed in the following way with PET. Imaging was started when the singles rate was below 2×10^6/s. The emission data were acquired at 180° rotation in 32 pre-set 30 second steps each. Decay and dead time correction were done before image reconstruction was accomplished. Because the PCD scans were later than the PET scans, activity loss of the same phantom in PCD was corrected to achieve the same amount of activity as that in PET scanning. The emission data were corrected by the uniform attenuation correction method. The OSEM algorithm, with the number of subsets equal to 32 and iterations equal to 1, was used for 2D image reconstruction. The data were rebinned into 96 projections and images were reconstructed in a 128 × 128 matrix with a Butterworth filter with a cutoff level of 0.35 cycle/pixel and order 2.

All PET and PCD images were acquired and reconstructed under conventional clinical conditions with slice thicknesses of 9.4 mm and 4.67 mm, respectively.

Image analysis

The aim of this study was to compare PCD versus dedicated PET studies, and the dedicated PET data were used as the gold standard. PET and PCD images were interpreted independently by two radiologists. A target was defined as a focus of increased ^{18}F uptake above the intensity of the surrounding activity. Targets were analyzed visually and semi-quantitatively. In the visual analysis, increased ^{18}F sodium fluoride solution was considered to be a hot spot. In the semi-quantitative analysis, regions

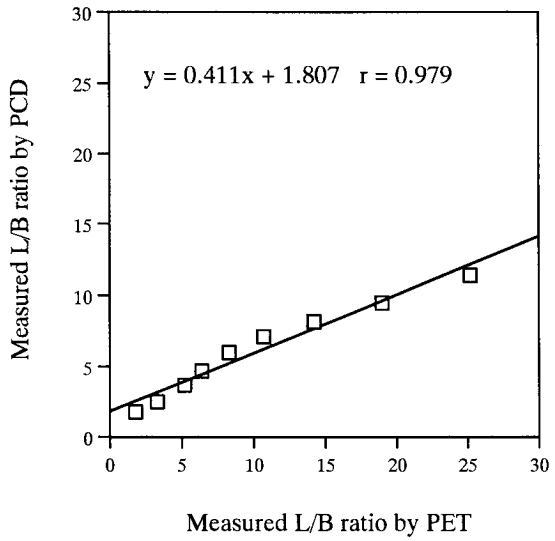

Fig. 3 Plot between L/B ratios measured on the 2D PET and PCD images, in the case of lesion diameter is 36.9 mm, respectively. Cross calibration line of L/B ratio between PET and PCD was achieved by the plot line.

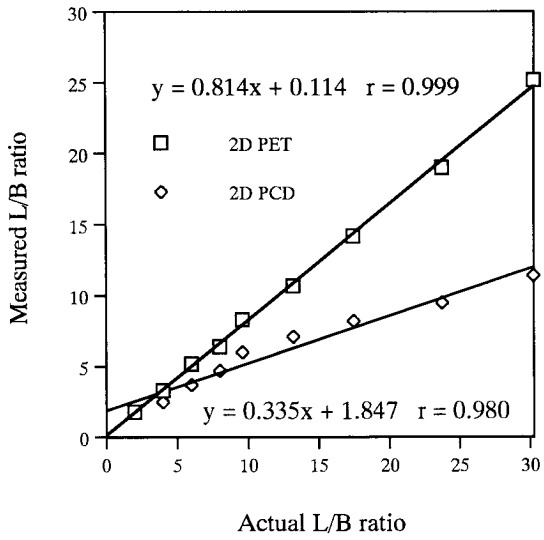

Fig. 4 Relationship between measured L/B ratios of PET and PCD and actual L/B ratio, in the case of lesion diameter is 36.9 mm, respectively. Significant positive correlations were observed between measured L/B ratio and actual L/B ratio in both PET and PCD.

of interest (ROI) analysis was employed to examine the quantitative values in PET and PCD reconstructed images. ROIs, 6 pixels in size, were drawn on the hot spots corresponding to the position and size of the targets on CT images. The highest point of radioactivity was included in these ROIs. A 30 mm diameter ROI was marked on the center of the phantom for background counts. The L/B ratio was defined as mean pixel counts in target/mean pixel counts in the background, and it was calculated for all hot spots in the PET and PCD images which were used to compare the semi-quantification in the PET and PCD methods. Detectability was defined as the ability to detect the target and was calculated as number of positive targets/total targets.

Statistical analysis

The L/B ratios was obtained by linear regression analysis. Statistical analysis of difference the p value was performed by Student's t-test. A $p < 0.05$ denoted the presence of a statistically significant difference.

RESULTS

An example of the hot spot phantom images of PET and PCD with the actual L/B ratio: 8.0 is given in Figure 1. The hot spots, ranging in diameter from 10.6 mm to 36.9 mm, are clearly identified with PET and PCD, but compared with PET image, the image quality of the background part of PCD image is quite inferior. The partial volume effect (PVE) in PET and PCD were investigated and Figure 2 shows PVE in PET and PCD with actual L/B ratios ranging from 2.0 to 30.3. The PEV in PCD is obviously inferior to that in PET. The measured L/B ratio was underestimated in PCD, compared to that in PET with the same actual L/B ratio, by 54.8% (target size: 36.9 mm) to 10% (target size: 4.4 mm) low difference, especially with the lesion size increasing. The relationships between the L/B ratios calculated on the 2D PET and PCD images were examined and the data for a lesion diameter of 36.9 mm are shown (Fig. 3). There was a strong positive correlation between the measured L/B ratios in PET and PCD ($r = 0.979$, $p < 0.001$). The relationships between the L/B ratios calculated on the 2D PET and PCD images and the actual L/B ratio were also examined. The data for the hot spot diameter of 36.9 mm are shown as well as in Figure 4, which shows strong positive correlations for both PET and PCD ($r = 0.999$ and 0.980, $p < 0.001$), but the measured L/B ratio in PCD was significantly lower than that of PET. Table 2 summarizes the visual interpretation of hot spots ranging from 4.4 to 36.9 mm in diameter with actual L/B ratios ranging from 2.0 to 30.3 in PET and PCD images. If an actual L/B ratio was 8.0, hot spots more than 10.6 mm could be clearly identified with PCD imaging, but on the other hand, the same identification could be achieved with PET imaging even if an actual L/B ratio was only 4.0. The detectability of small hot spots in PET and PCD was found to be 77.8% (2D PET) versus 64.8% (2D PCD).

DISCUSSION

FDG-PET is increasingly used in neurologic, cardiac and oncologic diseases, especially in clinical oncology,[12–14] but the high cost of dedicated PET scanners and cyclo-

trons has been a major constraint to the clinical use of FDG PET. Recently the technology of camera-based PET imaging and coincidence gamma camera detection has become available, and several clinical papers reported the clinical application of the coincidence gamma camera, but further fundamental and detail study has been thought essential.[8]

In our previous study,[15] a 20-cm cylinder phantom PCD experiment was assessed and we found that the spatial resolution of PCD is comparable with that of dedicated PET (5.3 mm of PCD versus 4.26 mm of PET in FOV), whereas the count rate capability (8.0×10^3/s for PCD in the 2D mode versus 7.3×10^4/s for PET in the 2D mode), sensitivity (1.8 kcps/kBq/m*l* for PCD versus 7.98 kcps/kBq/m*l* for PET in the 2D mode) and scatter fraction (22% for PCD versus 13.1% for PET in the 2D mode) are the limiting factors for PCD compared with dedicated PET.

As further investigation in this study, we explored the correlation in detectability and semi-quantification of FDG-PET and FDG-PCD in detecting small hot lesions of various lesion sizes and lesion to background uptake ratios. The lesion detectability of a PCD phantom study was found comparable with that of dedicated PET i.e., 64.8% (2D PCD) versus 77.8% (2D PET), which is within the range of previously published clinical results for dual-head coincidence gamma cameras of 55–79%.[8,16] Besides the L/B ratio, lesion size is an important factor determining detectability. Lesion detectability for lesions < 10.6 mm was only 22.2% for PCD versus 44.4% for PET, compared with 86.1% for PCD versus 94.4% for PET for lesions ≥ 10.6 mm (Table 1). The greater the contrast between the lesion and the background, the easier it is to detect the lesion. On the basis of visual analysis, the detectability limitation for lesions ≥ 10.6 mm in PCD and PET was found to be ≥ 8.0 and ≥ 4.0 of the L/B ratio, respectively.

Since the L/B ratio is the only available index that can be used for quantification of PCD images, the L/B ratio was used to evaluate the quantification of PCD and PET images. Compared with dedicated PET, PCD shows strong PVE with a 10% to 54.8% count loss and the measured L/B ratio was significantly lower in the PCD studies than with dedicated PET, which was due to the inferior spatial resolution of PCD compared with that of PET, and also because of the high scattered and random events in the PCD system (Fig. 2). This was easily identified by the inferior image quality of PCD, compared with the PET image in Figure 1. For example, when the actual L/B ratio was 8.0, the measured L/B ratio was 6.4 in the PET image, in contrast to 4.7 in the PCD image for a target 36.9 mm in diameter.

In the semi-quantitative analysis of phantoms in this study, there was a significant positive correlation between measured L/B ratios in PCD and PET ($r = 0.979$, $p < 0.001$) (Fig. 3); and also measured L/B ratios in PCD and PET and actual L/B ratio were observed ($r = 0.980$ for PCD versus $r = 0.999$ for PET) (Fig. 4), which suggested similar quantitative capability of PCD in hot spot lesion detection. In both Figure 3 and Figure 4, the measured L/B ratio was not linear with the actual L/B ratio, and there was a little trend to increase in the measured L/B ratio when the actual L/B ratio was about 13.2 in PCD, which might be due to the count rate limitation of PCD. When the activity inside the phantom is high (for example, more than the actual L/B ratio = 13.2), the count rate capability of PCD would be limited.

PCD has several limitations that diminish image quality and semi-quantification, compared with dedicated PET. The percentage of scatter and random events is considerably higher than for dedicated PET in the two-dimensional mode. Our previous phantom study had shown that the scatter and random fraction of a 20-cm cylinder was 22% for PCD, whereas it was 13.1% for the dedicated PET.[15] If PCD is done with patient imaging, an even high percentage of scatter and random counts could be expected. On the other hand, pulse pile-up in the detector system limited the singles count rate that could be processed by PCD. These factors resulted in noticeably reduced image quality when the singles count rate exceeded approximately 2×10^6/s. Despite comparable spatial resolution, the smaller number of coincidence events and the higher fraction of scatter and random count showed why the L/B ratio was significantly lower in the PCD studies than with dedicated PET. In addition, the sensitivity of PCD was about four times lower than that in PET, but the scan time of PCD was exactly twice than of PET. This may also result in the decreasing of image quality and detectability due to the statistical noise. Further investigation to obtain optimum scan time is needed.

In this study, PCD and PET images were not scatter corrected. Better results might be achieved if scatter correction of PCD and PET were done.

CONCLUSIONS

FDG PCD yielded results comparable to those of FDG PET on visual analysis and semi-quantitative analysis in detecting hot spots in this phantom study. Nevertheless, semi-quantitative analysis with the L/B ratio of FDG PCD was inferior to that of FDG PET and the detectability of PCD in smaller hot spots was quite poor. It is expected that the superior results will be achieved if scatter correction of PCD and PET is done.

REFERENCES

1. Strauss LG, Clorius JH, Schlag P, Lehner B, Kimmig B, Engenhart R, et al. Recurrence of colorectal tumors: PET evaluation. *Radiology* 1989; 170: 329–332.
2. Okada J, Yoshikawa K, Itami M, Imaseki K, Uno K, Kuyama J, et al. Positron emission tomography using

fluorine-18-fluorodeoxyglucose in malignant lymphoma: a comparison with proliferative activity. *J Nucl Med* 1992; 33: 325–329.
3. Coleman RE. Revealing biochemistry in a single image. *J Nucl Med* 1995; 36 (9): 32N–33N.
4. Conti PS, Keppler JS, Halls JM. Positron emission tomography: a financial and operational analysis. *AJR* 1994; 162: 1279–1286.
5. Martin WH, Delbeke D, Patton JA, Hendrix B, Weinfeld Z, Ohana I, et al. FDG-SPECT: correlation with FDG-PET. *J Nucl Med* 1995; 36: 988–995.
6. Van Lingen A, Huijgens PC, Visser FC, Ossenkoppele GJ, Hoekstra OS, Martens HJ, et al. Performance characteristics of a 511-keV collimator for imaging positron emitters with a standard gamma-camera. *Eur J Nucl Med* 1992; 19: 315–321.
7. Drane WE, Abbott FD, Nicole MW, Mastin ST, Kuperus JH. Technology for FDG SPECT with a relatively inexpensive gamma camera. Work in progress. *Radiology* 1994; 191: 461–465.
8. Shreve PD, Steventon RS, Deters EC, Kison PV, Gross MD, Wahl RL. Oncologic diagnosis with 2-[fluorine-18]fluoro-2-deoxy-D-glucose imaging: dual-head coincidence gamma camera versus positron emission tomographic scanner. *Radiology* 1998; 207: 431–437.
9. Zhang H, Inoue T, Alyafei S, Tian M, Oriuchi N, Endo K. Tumor detectability in 2-dimensional and 3-dimensional positron emission tomography using SET-2400W: A phantom study. *Nucl Med Commun* 2001; 22: 305–314.
10. Lewellen TK, Miyaoka RS, Swan WL. PET imaging using dual-headed gamma cameras: an update. *Nucl Med Commun* 1999; 20: 5–12.
11. Tanaka G. Japanese Reference Man 1988. III: Masses of organs and tissues and other physical properties. *Nippon Igaku Hoshasen Gakkai Zasshi* 1988; 48: 509–513.
12. Kuhl DE, Wagner HN, Alavi A, Coleman RE, Gould KL, Larson SM, et al. Positron emission tomography (PET): clinical status in the United States in 1987. *J Nucl Med* 1988; 29: 1136–1143.
13. Al-Aish M, Coleman RE, Larson SM, Barrio J, Brodack J, Brooks D, et al. Advances in clinical imaging using positron emission tomography. September 14–16, 1988. National Cancer Institute Workshop Statement. *Arch Intern Med* 1990; 150: 735–739.
14. Conti PS, Lilien DL, Hawlay K, Keppler J, Grafton ST, Bading JR. PET and (^{18}F)-FDG in oncology: a clinical uptake. *Nucl Med Biol* 1996; 23: 717–735.
15. Alyafei S, Inoue T, Zhang H, Oriuchi N, Koyama K, Endo K. Performance characteristics of PCD system in Axial filter (2D) and Open frame (3D) acquisition mode. *KAKU IGAKU (Jpn J Nucl Med)* 1999; 38: 615. (abstract)
16. Delbeke D, Patton JA, Martin WH, Sandler MP. FDG PET and dual-head gamma camera positron coincidence detection imaging of suspected malignancies and brain disorders. *J Nucl Med* 1999; 40: 110–117.